

## Resonant Raman scattering induced by excitons bound to nitrogen impurities in GaP:N

A. Frommer and E. Cohen

*Department of Physics and Solid State Institute, Technion-Israel Institute of Technology, Haifa 32000, Israel*

Arza Ron

*Department of Chemistry and Solid State Institute, Technion-Israel Institute of Technology, Haifa 32000, Israel*

(Received 27 February 1992; revised manuscript received 20 August 1992)

A study of the resonant Raman scattering (RRS) by optical phonons that is induced by excitons bound to isoelectronic nitrogen impurities in GaP is presented. Strong Raman lines are observed under resonant excitation into the inhomogeneously broadened 1S exciton band, at liquid He temperatures. They involve the  $LO_{\Gamma}$ ,  $TO_{\Gamma}$  phonons and a nitrogen-induced, forbidden scattering by the zone-edge  $LO_x$  phonon. The  $LO_x$  RRS profile is shown to be a sum of contributions from the  $J=1$  state of all N-bound excitons weighted by their density and damping factors. The RRS is dominated by those N-bound excitons which are perturbed by distant background impurities. A model based on the measured density of N-bound exciton states and on the energy-dependent damping factor is presented and is found to account well for the observed  $LO_x$  RRS profile. The main damping processes are due to tunneling between the various N-bound exciton states. The resonant enhancement of the  $LO_{\Gamma}$ -phonon scattering by the N-bound excitons is measured as  $10^9$  times that of the pure GaP crystal.

### I. INTRODUCTION

The spectroscopic properties of excitons bound to isoelectronic nitrogen impurities in GaP are well known.<sup>1</sup> The 1S state is split by  $e-h$  exchange into an upper  $J=1$  state and a lower  $J=2$  state with the corresponding transitions which are denoted  $A$  and  $B$ , respectively. The  $J=1$  and  $J=2$  excitons differ in two respects that are relevant to this study. (a) The  $A$  line is dipole allowed and the  $B$  line is forbidden. (b) They couple differently to optical phonons. While both couple to zone-center  $TO_{\Gamma}$  and  $LO_{\Gamma}$  phonons, only the  $J=1$  state couples strongly to the zone-edge  $LO_x$  phonon. This can clearly be observed in the luminescence spectra such as those shown in Fig. 1. At  $T=2$  K the emission is due mostly to excitons in the  $J=2$  state, while at 4.2 K the  $J=1$  emission dominates and thus the different phonon sidebands associated with either the  $B$  or the  $A$  lines can be observed.

The dynamic processes that take place during the long radiative lifetime of the 1S excitons have been studied by two time-resolved spectroscopy methods. Molenkamp and Wiersma<sup>2</sup> have measured, by photon-echo experiments, the decay time of the  $J=1$  into the  $J=2$  state:  $\tau_{AB}=25$  psec at  $T=1.5$  K. This decay is an internal exciton process involving acoustic phonon emission. Brocklesby, Harley, and Plant<sup>3</sup> have used the saturation spectral hole-burning technique within the inhomogeneously broadened  $B$  line. They find that at  $T=1.5$  K, the spectral hole width corresponds to exciton dephasing times of the order of 800 psec. They interpret the dephasing process as due to  $J=2$  exciton tunneling (hopping) between different N sites, which takes place even for nitrogen concentrations as low as  $[N] \approx 10^{15} \text{ cm}^{-3}$ .

Tunneling between various types of nitrogen-bound excitons was studied by luminescence. For  $[N] \geq 2 \times 10^{17} \text{ cm}^{-3}$ , nitrogen pairs ( $NN_i$ ) (Refs. 4 and 5) or triplets<sup>4</sup> act as terminal states: excitons bound to single nitrogens

tunnel between these sites until they are trapped on  $NN_i$  sites. A statistical model of exciton transfer involving pairs and triplets was presented by Leroux-Hugon and Mariette.<sup>6</sup>

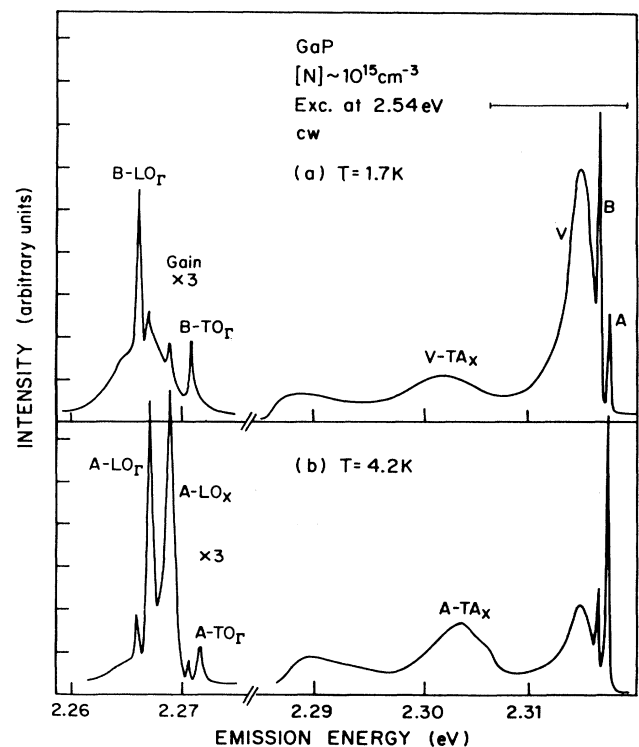


FIG. 1. Luminescence spectra of nominally undoped GaP:N. At 2 K the emission is due mostly to excitons in the  $J=2$  state ( $B$  line), while at 4.2 K the  $J=1$  emission dominates. Note the different optical-phonon sidebands. The spectral range, denoted by a horizontal bar in (a), is that of resonance excitation studied here.

The aim of this paper is to use the exciton damping factor that is measured by resonant Raman scattering (RRS) involving  $LO_X$  phonons, in order to study the dephasing mechanisms of N-bound excitons in the  $J=1$  state (at  $T=2$  K). It will be shown that exciton tunneling between those N sites, which give rise to the  $A$  and  $B$  lines, is the most important dephasing process even in nominally undoped samples (having only background impurities). Due to their large damping factor, excitons trapped on such N sites have a negligible contribution to the RRS cross section. It has been shown<sup>7</sup> that there is a band of N-bound excitons that are perturbed by distant impurities, in the spectral range just below the  $A$ - $B$  lines ( $V$  band in Fig. 1). These perturbed excitons have a larger binding energy than the unperturbed ones but their internal structure is preserved: they have the same  $J=1,2$  splitting and Zeeman splittings. In preliminary studies,<sup>8,9</sup> we showed that the RRS cross section involving the  $LO_X$  phonons is dominated by these states. In the present work we use time-resolved spectroscopy in order to distinguish between the RRS lines and the luminescence background. In this way we measured the  $LO_X$ -phonon RRS profile for GaP crystals with two different N concentrations:  $[N] \approx 10^{15}$  and  $10^{18} \text{ cm}^{-3}$ . We show that in both cases the RRS is most intense when excited in the  $V$ -band spectral range. We show that the observed RRS profiles are well explained by a model based on the density of perturbed N-bound exciton states and their energy-dependent damping factor.

The paper is laid out as follows. The experimental procedure and results are detailed in Sec. II. Section III details the model of  $LO_X$  phonon RRS cross section and we fit it to the experimentally observed scattering profile. In Sec. IV we estimate the overall enhancement of the RRS cross section by the N-bound excitons. A short summary concludes this paper.

## II. EXPERIMENTAL PROCEDURE AND RESULTS

Two GaP crystals were investigated; both were grown by vapor transport. One was nominally undoped but contained a background nitrogen concentration of  $[N] \sim 10^{15} \text{ cm}^{-3}$  (as estimated from the absorption strength of the  $A$  line). The other was doped to a level of  $[N] \sim 2 \times 10^{18} \text{ cm}^{-3}$ . All the spectroscopic studies were done with the crystals immersed in liquid He at  $T=2$  K. The excitation was done with a cw dye laser followed by an acousto-optic modulator producing pulses of  $\sim 50$ -nsec width at a repetition rate of  $\sim 100$  kHz. The spectral range of the excitation is marked in Fig. 1 by a horizontal bar. The light emitted from the crystals was dispersed through a double spectrometer (resolution of 0.05 meV). The signal was analyzed by a gated photon counter with a time resolution of 5 nsec. In order to differentiate the RRS from the luminescence for a given excitation energy, each spectrum was taken (with a gate of 50 nsec) at two different times: (a) coincident with the laser pulse (this spectrum contains both the RRS and the luminescence); (b) delayed by 50 nsec with respect to the laser pulse (this spectrum contains only the luminescence). Figure 2 shows two such examples of time-resolved spectra taken

for each one of the crystals under study. The spectra marked  $a$  and  $d$  were taken coincident with the laser pulse while  $b$  and  $e$  were delayed. All were monitored in the range of the optical-phonon sidebands with resonant excitation within the  $V$  band. The delayed spectrum was subtracted from the prompt response one after a correction was made for the overall luminescence intensity decay with time. The resulting spectra for the two crystals are shown in Figs. 2(c) and 2(f). These spectra are then taken as the net Raman scattering involving the transverse (denoted  $l - TO_T$  in Fig. 2) and longitudinal ( $l - LO_T$ ) phonons of the Brillouin zone center, as well as the longitudinal optical phonon of the zone edge ( $l - LO_X$ ). A series of spectra obtained by this subtraction method for different excitation energies yields the Raman scattering profile. Our interest in this study is in the scattering involving the  $LO_X$  phonon. Its experimentally observed RRS profiles for the two crystals under study are shown in Figs. 3(b) and 3(c).

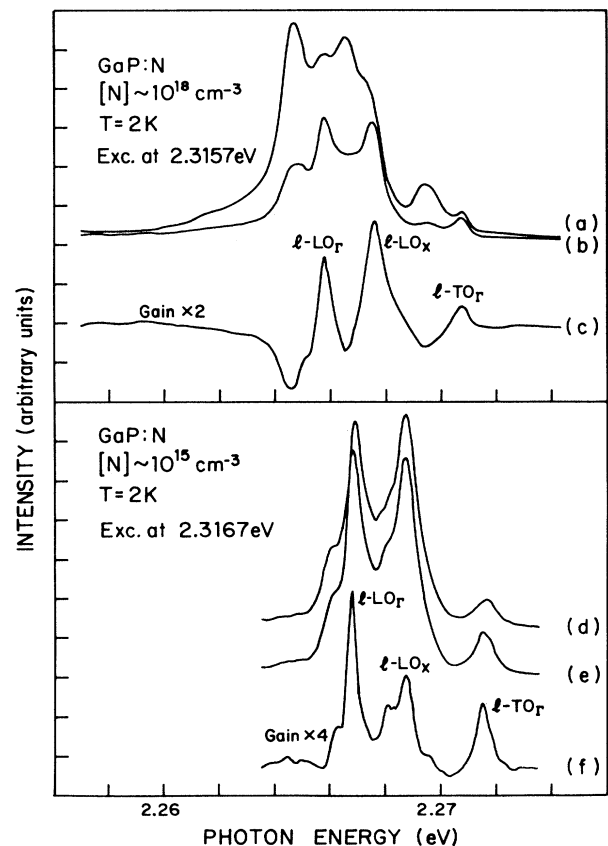


FIG. 2. Time-resolved photoluminescence spectra for two samples of GaP:N with different  $[N]$ . For the sample with  $[N] \sim 10^{18} \text{ cm}^{-3}$ , the spectra are the following: (a) is taken with a time gate coincident with the laser pulse, (b) is taken with the time gate right after the end of the laser pulse, and in (c) the RRS spectrum is obtained by subtracting spectra (b) and (c). The corresponding spectra for the sample with  $[N] \sim 10^{15} \text{ cm}^{-3}$  are (d), (e), and (f).

### III. RESONANT-RAMAN-SCATTERING PROFILE AND EXCITON DAMPING

The  $LO_X$  RRS is observed only in the spectral range of the N-bound exciton. In the absence of nitrogen impurities the  $LO_X$  scattering is forbidden and thus we conclude that it is induced by the nitrogen impurities and a

$$K_{\alpha\beta}(E_l, E_s) = \langle g, 1_X | P_\alpha | (J=1, M_J), 1_X \rangle \langle (J=1, M_J), 1_X | H_{el}(LO_X) | (J=1, M_J), 0_X \rangle \\ \times \langle (J=1, M_J), 0_X | P_\beta | g, 0_X \rangle \{ [E_l - E - i\Gamma(E)][E_s - E - i\Gamma(E)] \}^{-1}. \quad (1)$$

$E_l(E_s)$  is the incoming (outgoing) photon energy,  $E_l - E_s = \hbar\omega_X$ ,  $E \equiv E(J=1, M_J)$  is the energy of the  $(J=1, M_J)$  state of the N-bound exciton, and  $g$  is the crystal ground state.  $\Gamma(E)$  is the damping factor, which is a measure of the dephasing rate of the  $J=1$  state with energy  $E$ . Let  $\rho_{J=1}(E)$  be the density of the  $J=1$ , N-bound excitons. Then the  $LO_X$  RRS cross section at an incoming (laser) energy  $E_l$  is given by<sup>10</sup>

$$\sigma_X(E_l) = \tilde{A} \int |K_{\alpha\beta}(E_l, E_s)|^2 \rho_{J=1}(E) dE \\ = A \int \frac{\rho_{J=1}(E)\Gamma(E)}{(E_l - E)^2 + \Gamma^2(E)} dE. \quad (2)$$

Since we study only the relative intensity of the  $LO_X$  RRS (namely, the scattering profile), we have lumped together in the constant  $A$  all the factors that are independent of  $E$  and  $E_l$ . We assume that the transition dipole matrix elements such as  $\langle g | P | (J=1, M_J) \rangle$  as well as the exciton- $LO_X$ -phonon interaction matrix element  $\langle (J=1, M_J), 1_X | H_{el}(LO_X) | (J=1, M_J), 0_X \rangle$ , are independent of the particular N-bound exciton (see below). We thus have to determine  $\rho_{J=1}(E)$  and  $\Gamma(E)$ .

The observed Raman profile in the spectral range of the  $V$  band, those N-bound excitons that are perturbed by distant impurities. There is a negligible scattering intensity at the  $A$ -line energy ( $E_A$ ). This is the case for the two crystals under study, even though they differ by three orders of magnitude in the nitrogen concentration. It is thus clear that in spite of the large value of  $\rho_{J=1}(E_A)$ , the damping factor  $\Gamma(E \sim E_A)$  is also very large.

The density of exciton states in the spectral range of the  $V$  band cannot be measured by absorption as it is too weak. We thus use the luminescence spectrum at  $T=2$  K, and fit the low-energy tail of the  $V$  band to an exponentially decreasing function for the density of states. This is a plausible assumption since the perturbing impurities are randomly distributed. The probability of finding a perturbing impurity close to a N atom is decreasing with decreasing distance between them. Therefore, resonant tunneling and phonon-assisted intersite transfer between the states down in the tail are negligible. Thus these are terminal states and the tail of the luminescence spectrum can be taken as a good approximation to the density of states. This distribution starts at the  $B$  line

minimal concentration of  $[N] \sim 10^{15} \text{ cm}^{-3}$  is required in order to observe it. The RRS profile of this phonon can then be used to study the dynamics of the N-bound exciton. The  $LO_X$  phonon couples only to the  $J=1$  state of the N-bound exciton and this is the case for the perturbed N-bound excitons ( $V$  band) as well.<sup>8</sup> Therefore only this state contributes significantly to the scattering matrix element, which can then be written as follows.<sup>8</sup>

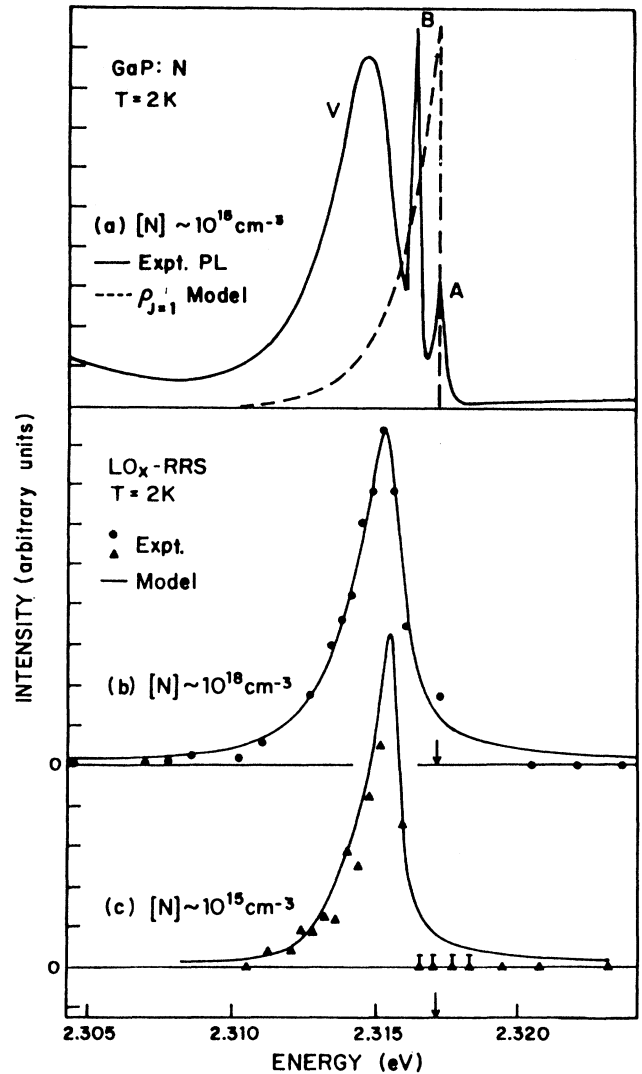


FIG. 3. (a) Photoluminescence spectrum (PL) and the model density of  $J=1$ , perturbed N-bound exciton states. (b) The experimental  $LO_X$ -phonon RRS intensities and the calculated cross-section profile for the high  $[N]$  sample. (c) The same for the low  $[N]$  sample. The bars indicate the measured error in the spectral range of the  $A$  line. This error is due to resonant luminescence, which dominated the spectrum in this energy range.

where it has its peak value:

$$\rho_{J=2}(E) = \rho_0 \exp[(E - E_B)/E_0] \quad (E < E_B). \quad (3)$$

The fit yields  $E_0 = 1.35$  meV. Since the exciton states involved in the  $LO_X$  RRS are those of  $J=1$  ( $A'$ -line), we obtain the density of these states from that of the associated  $J=2$  states [Eq. (3)]:

$$\rho_{J=1}(E) = \rho_0 \exp[(E - E_A)/E_0] \quad (E < E_A). \quad (4)$$

This function is plotted in Fig. 3(a). Following the model of Leroux-Hugon and Mariette,<sup>6</sup> the distant, perturbing impurities that give rise to the  $V$  band are the nitrogen impurities themselves. Then,  $\rho_0 \propto \rho_N^2$  (here  $\rho_N$  is the nitrogen concentration [N]). For the [N]  $\sim 10^{18}$  sample this model is reasonable, but we shall use it also for the lower concentration sample. As will be shown later, the model fitting to the experimental Raman profiles justifies this assumption.

$$\begin{aligned} \Gamma(E) = & \bar{B} |M(E - E_A)|^2 \rho(E_A) e^{(E - E_A)/KT} + \bar{B} \int_E^{E_A} |M(E - E_i)|^2 \rho_{J=1}(E_i) e^{(E - E_i)/KT} dE_i \\ & + \tilde{C} \rho_{J=1}(E) + D \int_{E_i}^E W_i(E - E_i) dE_i. \end{aligned} \quad (5)$$

In this expression the first term accounts for the thermally activated transfer from a perturbed N-bound exciton state with energy  $E$  to the  $A$  line and the second term to thermal activation to any of the other perturbed states with higher energy  $E < E_i < E_A$ .  $M(E - E_i)$  is the matrix element of the exciton-acoustic phonon interaction. It is included in the terms of the phonon-assisted transfer rate that depends on the energy separation of the states involved in the transfer process.  $\bar{B}$  contains all the other factors that are independent of the energy and of the density of states. The dominant interaction with low-energy, zone-center, longitudinal acoustic phonons is the deformation-potential (DP) interaction,<sup>12</sup> for which we have<sup>13</sup>

$$|M^{DP}(q)|^2 = \frac{\hbar q}{2g_s v_l} (\epsilon_c \alpha_e - \epsilon_v \alpha_h)^2. \quad (6)$$

$q = \Delta E / \hbar v_l$  is the wave vector of the emitted zone-center acoustic phonon,  $\Delta E = E - E_i$  is its energy, and  $v_l$  is the appropriate sound velocity.  $\epsilon_c$  is the (averaged) conduction band DP ( $\epsilon_v$  is the corresponding one for the valence band).  $g_s$  is the crystal density.

$$\alpha_{e,h} = \left[ 1 + \left( \frac{m_{h,e} q a_B}{2M_X} \right)^2 \right]^{-2}, \quad (7)$$

where  $m_e$  ( $m_h$ ) is the electron (hole) effective mass,  $M_X$  is the exciton translational mass, and  $a_B$  is its Bohr radius. Near the zone center  $|M(\Delta E)|^2 \sim \Delta E$  and therefore it is possible to neglect this linear energy dependence with respect to the exponential energy dependence of the Boltzmann factor.

The third term of Eq. (5) corresponds to resonant tun-

ing of excitons with the same energy. Since we do not have any knowledge on the distribution of the distances between nitrogen atoms, we assume that the resonant tunneling is proportional to the density of exciton states that is given in Eq. (4). The last term of Eq. (5) accounts for the acoustic phonon-assisted tunneling into lower-energy states in the  $V$  band.  $E_i$  is a lower bound for the energies in the  $V$  band and  $W_i$  is the tunneling rate. Since the density of perturbed exciton states is very low, we shall neglect the two terms that correspond to acoustic phonon-assisted tunneling processes within states in the  $V$  band [the second and last terms of Eq. (5)]. We then end up with the following approximate expression for the damping factor:

$$\Gamma(E) = B \rho_N e^{(E - E_A)/KT} + C \rho_N^2 e^{(E - E_A)/E_0}. \quad (8)$$

Figure 4 shows the dependence of each of the terms in Eq. (8) on the perturbed N-bound exciton energy  $E$ . The ratio  $B/C$  is a free parameter (to be determined experimentally), which is independent of energy and of the nitrogen concentration. A fit of Eq. (8) to the experimentally observed RRS profile of the crystal with [N]  $\sim 10^{18}$   $\text{cm}^{-3}$  is shown in Fig. 3(b) and it yields the value of  $B/C \sim 10^{21}$   $\text{cm}^3$ . Using this value, the calculated  $\Gamma(E)$  is shown in Fig. 4(c). We note that the thermally activated transfer of excitons into the  $A$  line (curve  $b$ ) is dominant above  $\sim 2.316$  eV, namely, 1 meV below the  $A$  line. This explains the sharp drop in  $\sigma_X(E_l)$  in the spectral range just below the  $A$  line. Using the same  $B/C$  ratio we then calculate  $\sigma_X(E_l)$  for the sample with [N]  $\sim 10^{15}$   $\text{cm}^{-3}$ . An excellent fit is obtained [Fig. 3(c)], which supports our assumption that the dephasing process due to resonant tunneling is indeed proportional to  $\rho_N^2$ .

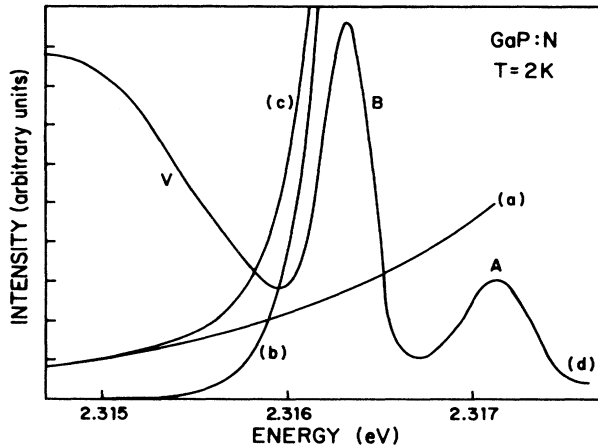


FIG. 4. Model calculations. The dependence of the two dominant damping factors on the N-bound exciton energy: (a) tunneling between perturbed nitrogen sites and (b) thermal activation into the unperturbed N-bound state. The sum of these two damping factors, weighted to give the best fit to the observed RRS profile [Eq. (8)], is given in (c). In (d) we show the experimental luminescence spectrum in order to indicate the pertinent exciton lines.

#### IV. NITROGEN-ENHANCED RRS INTENSITY

We can estimate the enhancement of the scattering cross section by the nitrogen impurities in the following way: We measure the ratio between the RRS intensity of the  $LO_{\Gamma}$  phonon mediated by N-bound excitons ( $I_N$ ) and that mediated by all other electronic states that are far removed from the  $A$  line ( $I_0$ ).  $\sigma_N$  and  $\sigma_0$  are the corresponding scattering cross sections. Generally, the scattering intensity is given by the product of the cross section and the density of scattering centers. Then we can write

$$\frac{\sigma_N}{\sigma_0} = \frac{I_N}{I_0} \frac{\text{density of unit cells}}{\text{density of perturbed N-bound exciton states}} \quad (9)$$

We measure for the heavily doped GaP:N crystal ( $[N]$

$\sim 10^{18} \text{ cm}^{-3}$ ):  $I_N/I_0 \sim 65$ , where  $I_N$  is taken at the peak of the  $LO_{\Gamma}$  RRS profile and  $I_0$  is measured  $\sim 10 \text{ meV}$  below it. The density of perturbed N-bound exciton sites that have the largest contribution to the  $LO_{\Gamma}$  RRS (Ref. 8) is estimated to be  $\sim 10^{15} \text{ cm}^{-3}$ . The density of unit cells is  $5 \times 10^{22} \text{ cm}^{-3}$  and thus  $\sigma_N/\sigma_0 \sim 10^9$ . Such a large enhancement by excitons bound to impurities has been previously reported<sup>14</sup> for donor-bound excitons in GaAs and CdTe.

#### V. SUMMARY

In this paper we studied the effects of nitrogen-bound excitons on the phonon Raman scattering in GaP:N. The scattering involving the zone-edge  $LO_X$  phonon is induced by the N impurities and is thus used as a probe of the dynamic processes that control the N-bound excitons. We show that only the  $J=1$  excitonic state induces the scattering and that due to its damping, only excitons bound to slightly perturbed N sites contribute significantly to the RRS. A model of exciton dephasing (as a source of damping) is presented. It is based on two main dynamic processes: thermal activation of the perturbed N bound excitons into the  $A$  line and resonant tunneling of excitons with the same energy. The model uses only the ratio of the preexponential factors (of these two processes) as a free parameter. In addition, the density of perturbed N-bound exciton states is extracted from the photoluminescence spectrum. A very good fit to the observed RRS profile is obtained for two crystals with  $[N] \sim 10^{15} \text{ cm}^{-3}$  and  $10^{18} \text{ cm}^{-3}$ . This demonstrates the adequate description of dephasing in one of the most studied bound-exciton systems in the field of semiconductor spectroscopy. We also compare the  $LO_{\Gamma}$ -phonon-scattering intensity induced by the N-bound excitons with that of all other electronic states and find that the former is  $\sim 10^9$  times stronger than the latter.

#### ACKNOWLEDGMENTS

This study was supported by the United States-Israel Binational Science Foundation (BSF), Jerusalem, Israel, and was done at the Center for Advanced Opto-Electronics Research in the Technion.

<sup>1</sup>P. J. Dean and D. C. Herbert, in *Excitons*, edited by K. Cho (Springer, Berlin, 1979), p. 55.  
<sup>2</sup>L. W. Molenkamp and D. A. Wiersma, *Phys. Rev. B* **32**, 8108 (1985).  
<sup>3</sup>W. S. Brocklesby, R. T. Harley, and A. S. Plant, *Phys. Rev. B* **36**, 7941 (1987).  
<sup>4</sup>P. J. Wiesner, R. A. Street, and H. D. Wolf, *Phys. Rev. Lett.* **35**, 1366 (1975).  
<sup>5</sup>P. J. Wiesner, R. A. Street, and H. D. Wolf, *J. Lumin.* **12/13**, 265 (1976).  
<sup>6</sup>P. Leroux-Hugon and H. Mariette, *Phys. Rev. B* **30**, 1622

(1984).

<sup>7</sup>D. Gershoni, E. Cohen, and Arza Ron, *J. Lumin.* **34**, 83 (1985).  
<sup>8</sup>D. Gershoni, E. Cohen, and Arza Ron, *J. Lumin.* **38**, 230 (1987).  
<sup>9</sup>A. Frommer, Y. Garini, Arza Ron, and E. Cohen, *J. Lumin.* **45**, 9 (1990).  
<sup>10</sup>R. M. Martin and L. M. Falicov, in *Light Scattering in Solids*, edited by M. Cardona, Topics in Applied Physics Vol. 8 (Springer-Verlag, Berlin, 1980), p. 79.  
<sup>11</sup>D. Gershoni, E. Cohen, and Arza Ron, *Phys. Rev. B* **37**, 4577 (1988).

<sup>12</sup>This is based on our study of the acoustic-phonon sideband associated with the excitons bound to nitrogen pairs [A. Frommer, E. Cohen, and A. Ron (unpublished)].

<sup>13</sup>R. G. Ulbrich and C. Weisbuch, in *Light Scattering in Solids*,

edited by M. Cardona and G. Guntherodt (Springer-Verlag, New York, 1982), Vol. 3, p. 207.

<sup>14</sup>R. G. Ulbrich, N. Van Hieu, and C. Weisbuch, *Phys. Rev. Lett.* **46**, 53 (1981).